4-16-2019

Tsunamigenic Splay Faults Imply a Long-Term Asperity in Southern Prince William Sound, Alaska

L. M. Liberty
Boise State University

D. S. Brothers
U.S. Geological Survey

P. J. Haeussler
U.S. Geological Survey

Geophysical Research Letters

RESEARCH LETTER
10.1029/2018GL081528

Tsunamigenic Splay Faults Imply a Long-Term Asperity in Southern Prince William Sound, Alaska

L. M. Liberty[1], D. S. Brothers[2], and P. J. Haeussler[3]

[1]Department of Geosciences, Boise State University, Boise, ID, USA, [2]Pacific Coastal and Marine Science Center, U.S. Geological Survey, Santa Cruz, CA, USA, [3]U.S. Geological Survey, Anchorage, AK, USA

Key Points:
- Megathrust splay faults that surface near Prince William Sound, Alaska, show clear evidence for repeated sea floor uplift
- The spatial and temporal splay fault character indicates a persistence of a plate boundary asperity related to the subducted Yakutat terrane
- Tsunamis generated from coseismic fault motion during future megathrust earthquakes will show repeating patterns as during the 1964 event

Supporting Information:
- Supporting Information S1

Correspondence to:
L. M. Liberty,
lliberty@boisestate.edu

Citation:
Liberty, L. M., Brothers, D. S., & Haeussler, P. J. (2019). Tsunamigenic splay faults imply a long-term asperity in southern Prince William Sound, Alaska. *Geophysical Research Letters*, *46*, 3764–3772. https://doi.org/10.1029/2018GL081528

Received 30 NOV 2018
Accepted 19 MAR 2019
Accepted article online 25 MAR 2019
Published online 15 APR 2019

Abstract Coseismic slip partitioning and uplift over multiple earthquake cycles is critical to understanding upper-plate fault development. Bathymetric and seismic reflection data from the 1964 M*w*9.2 Great Alaska earthquake rupture area reveal sea floor scarps along the tsunamigenic Patton Bay/Cape Cleare/Middleton Island fault system. The faults splay from a megathrust where duplexing and underplating produced rapid exhumation. Trenchward of the duplex region, the faults produce a complex deformation pattern from oblique, south-directed shortening at the Yakutat-Pacific plate boundary. Spatial and temporal fault patterns suggest that Holocene megathrust earthquakes had similar relative motions and thus similar tsunami sources as in 1964. Tsunamis during future earthquakes will likely produce similar run-up patterns and travel times. Splay fault surface expressions thus relate to plate boundary conditions, indicating millennial-scale persistence of this asperity. We suggest structure of the subducted slab directly influences splay fault and tsunami generation landward of the frontal subduction zone prism.

Plain Language Summary We identify prominent sea floor scarps that show a similar pattern of tectonic uplift over the past 20 to 30 subduction zone earthquakes in the western Prince William Sound area of Alaska. Our results suggest that plate boundary conditions have been fixed through many earthquake cycles and that subducted plate boundary conditions influence sea floor uplift patterns. We conclude that tsunami patterns observed during the 1964 earthquake will likely repeat to reproduce run-up and travel time observations. Mapping structures along plate boundaries is critical to understanding tsunami sources in subduction zones.

1. Introduction

Thrust faults that splay from a megathrust within subduction zone accretionary wedges can pose major seismic and tsunami hazards, yet little is known about the spatial and temporal controls on this family of faults. Surface ruptures during subduction zone earthquakes can highlight patterns of coseismic motion (e.g., Fujiwara et al., 2011; Henstock et al., 2006), paleoseismic and geodetic observations can provide estimates of recurrence intervals and patterns of uplift/subsidence (e.g., Atwater & Hemphill-Haley, 1997; Cisternas et al., 2005; Saillard et al., 2017; Shennan et al., 2014; Sieh et al., 2008), and thermochronology measurements can provide regional uplift rates over thousands of earthquake cycles (e.g., Enkelmann et al., 2015; Ferguson et al., 2015; Haeussler et al., 2015). However, detailed slip partitioning and uplift patterns over multiple earthquake cycles remains unknown. Constraints on these parameters are critical to understanding fault evolution, the relationship of faults to known plate boundary asperities or locked zones, the paleoseismic record, and tsunami genesis.

Using a tight grid of 40 sparker seismic profiles, coupled with new high-resolution sea floor imagery and legacy geophysical data, we characterize a complex fault system that developed by oblique and dip-slip shortening above a megathrust. These faults lie within the primary rupture area of the 1964 M*w*9.2 Great Alaska earthquake, immediately outboard of the subducted Yakutat terrane boundary and offshore the Montague Island area of Prince William Sound (PWS; Figure 1). Given that the recurrence interval for large earthquakes is estimated at 500 to 600 years (Carver & Plafker, 2008; Shennan et al., 2014) and that ~50 mm/year of N30°W plate convergence is documented (Elliott et al., 2010), we examine Holocene uplift patterns or motion over the past 20 to 30 post-glacial earthquake cycles. From long-term uplift patterns and from 1964 earthquake observations, we suggest that much of the last 500 to 750 m of plate shortening was accommodated along a series of subparallel splay faults. As splay faults are a relatively common, albeit poorly known feature of accretionary complexes, our results provide a rare glimpse into surface-rupturing

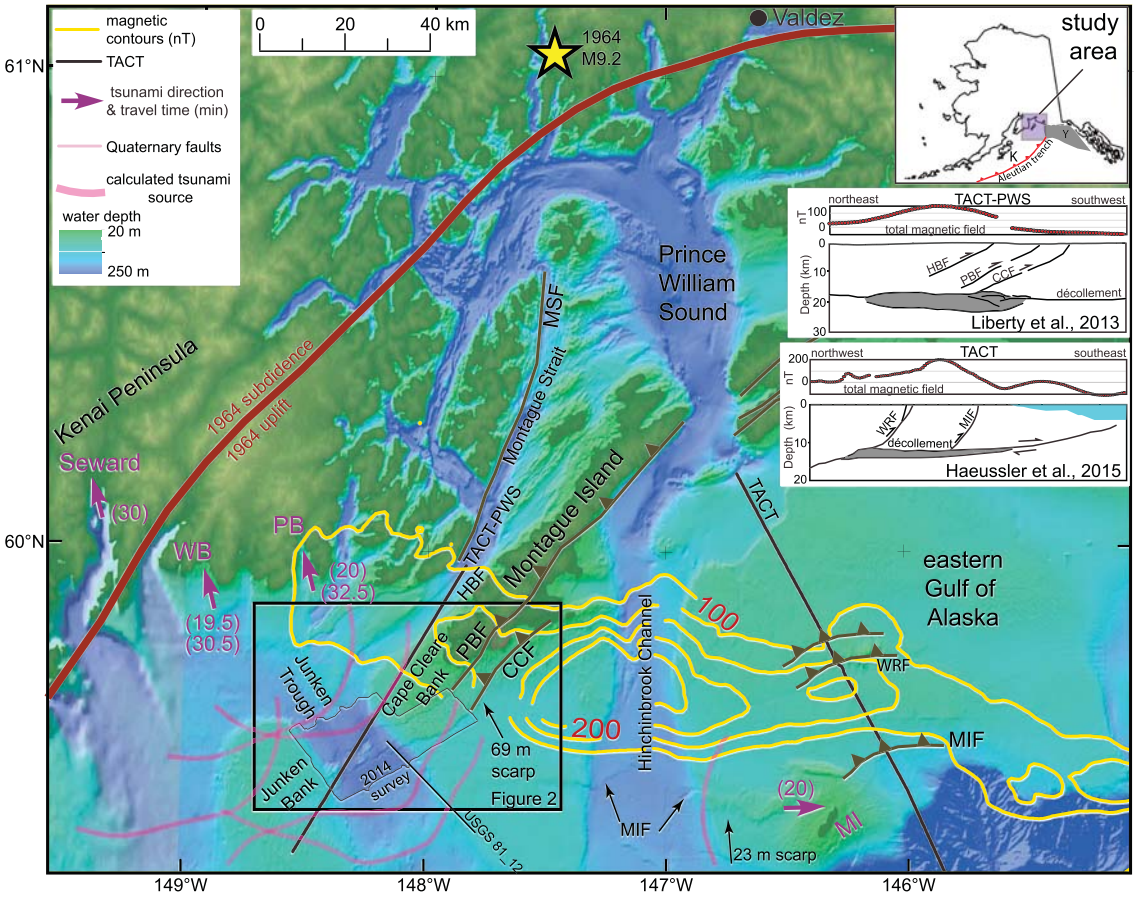

Figure 1. Bathymetric map of southern Alaska showing the epicentral area for the 1964 M*w*9.2 earthquake (yellow star), the hinge line between 1964 uplift from subsidence (red), significant 1964 surface rupturing faults (light red), magnetic contours (50-nT interval) that define the trailing edge of the subducted Yakutat terrane or SMA (yellow), select Trans-Alaska Crustal Transect (TACT) and U.S. Geological Survey seismic profile locations, 1964 tsunami run-up locations and directions (purple arrows), Plafker (1969) tsunami travel times (parentheses), and calculated source region (light purple lines). The inset map shows the study area, trench, and the nonsubducted portion of the Yakutat terrane (Y) and Kodiak Island (K). Two cross sections along TACT seismic profiles show key upper-plate interpretations, with shaded areas representing the crustal duplexing zone beneath a décollement. Select faults: PBF = Patton Bay fault, CCF = Cape Cleare fault; MIF = Middleton Island fault; MSF = Montague Strait fault; WRF = Wessels Reef fault; Other abbreviations: PB = Puget Bay; WB = Whidbey Bay; MI = Middleton Island. The Figure 2 box represents the zone of maximum surface/sea floor displacements documented during the 1964 earthquake (Liberty et al., 2013; Plafker, 1969). PWS = Prince William Sound.

processes. Despite the complexity of this fault system, the data show a pattern of persistent sea floor ruptures and growth faulting between regions with presumably lower shortening rates. We use bathymetric images to identify the tectonic tsunami sources from the 1964 earthquake and seismic data to refine the late Holocene deformation history of these splay faults.

2. The 1964 Great Alaska Earthquake

The 1964 M*w*9.2 earthquake ruptured an 800 km by 250 km area, causing tsunamis along the Gulf of Alaska coastline (Plafker, 1969). The earthquake initiated at ~25-km depth beneath northern PWS (Figure 1), and high moment release areas were identified near the southwest extent of Montague Island (Figure 2 and supporting information Figure S1) and immediately south of Kodiak Island (Christensen & Beck, 1994; Johnson et al., 1996). Release from the PWS asperity produced 21 m of horizontal surface displacement near the edge of the subducted Yakutat terrane (Plafker, 1969; Figures 1 and 2), where near-flat slab subduction and underthrusting was interpreted to intersect the steeper-dipping Pacific plate interface (Brocher et al., 1994; Kim et al., 2014). The region of inferred duplexing (Haeussler et al., 2015; Liberty et al., 2013) and maximum slip during the 1964 earthquake (Plafker, 1969) was coincident with the Slope Magnetic Anomaly (SMA) lineament that marks the southwestern edge of the subducting Yakutat terrane (Brocher et al.,

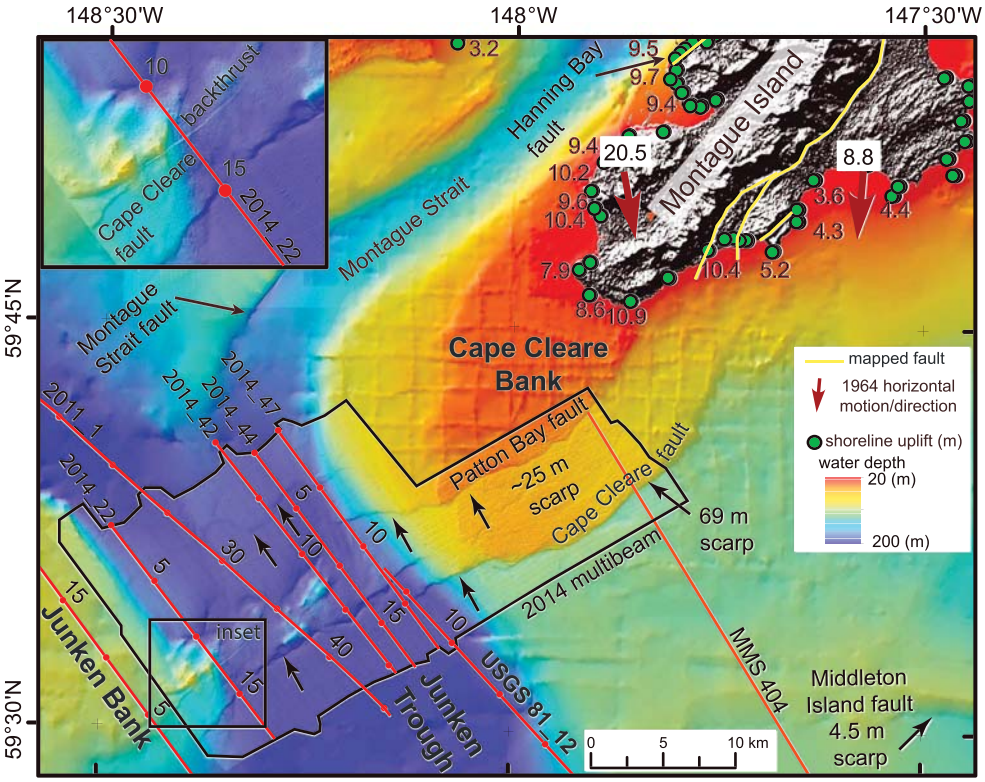

Figure 2. Bathymetric map with new multibeam survey that highlights lineaments related to the Patton Bay and Cape Cleare faults (black arrows). Select seismic profiles (red), 1964 shoreline uplift measurements in meters (green dots), and 1964 horizontal direction and motion in meters (red arrows) from 1964 earthquake (Plafker, 1969). Distances (in km) are labeled along each seismic profile. The waffle pattern on the Cape Cleare Bank bathymetry results from combining sparse (1929) and track line (1965) bathymetric survey. Inset map shows a portion of the Cape Cleare thrust and back-thrust best described by profile 2014_22 (Figure S5). Yellow lines are faults mapped by Plafker (1969). MMS = Mineral Management Services; USGS = U.S. Geological Survey.

1994; Bruns, 1983; Kim et al., 2014; Figure 1). The rupture lifted western Montague Island and the adjacent sea floor as much as 12 m along listric thrust faults that splay from a décollement (Liberty et al., 2013; Haeussler et al., 2015; Figure 1). Because little trenchward motion was recorded on Middleton Island in 1964 (Figure 1), Plafker (1969) concluded that horizontal shortening from this earthquake was accommodated almost entirely along faults that lie on the continental shelf. Few large (M > 5), post-1964 earthquakes have been recorded in the PWS area, which now appears to be completely locked (e.g., Freymueller et al., 2008; Zweck et al., 2002).

Immediately after the 1964 earthquake, tsunami run-up was documented at numerous sites on Kodiak Island, Kenai Peninsula, PWS, and Middleton Island (Plafker, 1969; Figure 1). Although submarine landslide-induced tsunamis were initiated along the deep fjord coastlines within minutes of ground shaking (e.g., Brothers et al., 2016; Haeussler et al., 2014; Parsons et al., 2014), the tectonic tsunami travel times ranged from about 20 min to many hours, indicating sources on the Alaskan continental shelf. While Plafker (1969) used travel times to infer that the tsunamis originated along the offshore extension of the Patton Bay fault system that surfaces on Montague Island (Figure 1), tsunami sources were not linked to specific sea floor scarps.

3. Methods and Data

Since the velocity of tsunami waves is directly proportional to water depth (Murty, 1977), we refine the Plafker (1969) tsunami travel distances using bathymetric survey data. Here we combine travel times from a run-up database (Plafker, 1969) with digital bathymetric data to identify sea floor scarps responsible for tsunami generation (Figure 1). Eyewitness accounts from Puget, Whidbey, and Resurrection Bays near

Seward suggest two tectonic sources caused wave run-ups that arrived approximately 20 and 30 min after the earthquake (Figure 1). Plafker (1969) noted a north-directed wave and upward first motion (assuming a direct travel path) for both Puget and Whidbey Bays, whereas the tsunami on Middleton Island originated from west of the island with a downward first motion.

To map faults and record slip history related to coseismic release of the PWS asperity, we conducted a high-resolution bathymetric and subbottom profiling survey around the Junken Trough (Figure S1). We chose this focus area due to its proximity to the splay faults with surface rupture during the 1964 earthquake (Figure 2). This glacially scoured cross-shelf trough likely has a near-continuous Holocene sedimentary record (e.g., Jakobsson et al., 2014) and is located adjacent to Montague Island.

Approximately 27 km^2 of multibeam bathymetry data were acquired aboard the Alaska Department of Fish and Game Vessel R/V Solstice with a Reson SeaBat 7111 (100 kHz; 301 beams). During data collection, tidal values were referenced to Mean Lower Low Water and soundings were edited and processed using Reson PDS2000 software. A final raster grid was created at 10-m cell spacing and loaded into ESRI ArcGIS and QPS Fledermaus for interpretation and comparison to earlier bathymetric data (Figure 2). Additionally, high-resolution single-channel seismic reflection profiles were simultaneously acquired using a 500-J SIG 2-Miile minisparker source (Balster-Gee et al., 2019). Acoustic frequencies between 150 and 750 Hz provided meter-scale resolution and penetration of up to 500 ms (~350-m depth). We complement these new data with legacy bathymetric and seismic data. Here we include the Boise State sparker profile 2011_1 (Liberty et al., 2013), the U.S. Geological Survey (USGS) airgun profile 81_12, and the Mineral Management Services (MMS) airgun profile 404. The USGS seismic profile, acquired in 1981, consisted of a 21.7-L air gun array, 50-m shot spacing, and a 2.4-km, 24-group streamer (Fruehn et al., 1999). The MMS profile, acquired in 1975, consisted of a 29.5-L air gun array and a 3.6-km 96-group streamer (Liberty, 2013). We depth converted sparker seismic profiles using a velocity of 1,500 m/s and airgun seismic profiles using stacking velocities obtained during processing.

Key horizons identified with our new seismic survey represent major changes in Holocene sediment deposition throughout the PWS and Gulf of Alaska regions (Finn et al., 2015; Haeussler et al., 2015; Liberty et al., 2013). With our data set, we identify three seismic stratigraphic packages above acoustic basement (Figures 3 and S2 to S5). The uppermost sequence, unit I, has well-defined continuous horizontal reflectors that underlie the sea floor. Unit I is usually not present beneath the shallow shelf region, and it is commonly 10 to 30 m thick in the Junken Trough and other cross-trough regions along the Gulf of Alaska (e.g., Carlson, 1989). We interpret this unit as related to the millennial-scale deposition of fine-grained, suspended sediment derived primarily from the Copper River delta (Jaeger et al., 1998; Kuehl et al., 2017).

Unit II has a clear angular unconformity at its base, often marked by a thin acoustically transparent basal layer. Above the base, the unit features moderate-amplitude parallel reflectors and ranges from 25 to 50 m thick. We interpret this unit as being deposited soon after glaciers retreated from their Last Glacial Maximum (LGM) position, likely between 17 and 14 ka (Kopczynski et al., 2017; Mann & Peteet, 1994; Misarti et al., 2012). Deposition of this unit was mostly focused within the deep troughs that lie below the early Holocene sea levels (Shugar et al., 2014). We infer these sediments were deposited on a surface that was abraded and leveled during LGM ice advances, and we reconstruct the Holocene deformation history of the active faults with this assumption.

Unit III consists of sediments that lie below the LGM unconformity and above Cenozoic acoustic basement. The acoustic character of unit III strata is variable, with some sediment packages having strong parallel reflectors and others with lateral variability and weak or no coherent reflections. The unit III strata are likely contemporaneous with the late Pliocene/early Pleistocene Yakataga Formation of Middleton Island (Lagoe et al., 1993; Taliaferro, 1932).

4. Accretionary Wedge Thrusts

4.1. Patton Bay Fault

The most dramatic expression of surface fault rupture in the 1964 earthquake was along the Patton Bay fault system, identified on southern Montague Island (Plafker, 1969). The system of faults includes en echelon, 45–70° northwest-dipping northeast-trending reverse faults with up to 8 m of uplift in response to 12 m of south-directed differential shortening across the Patton Bay fault (Figure 2). As inferred by Plafker (1969),

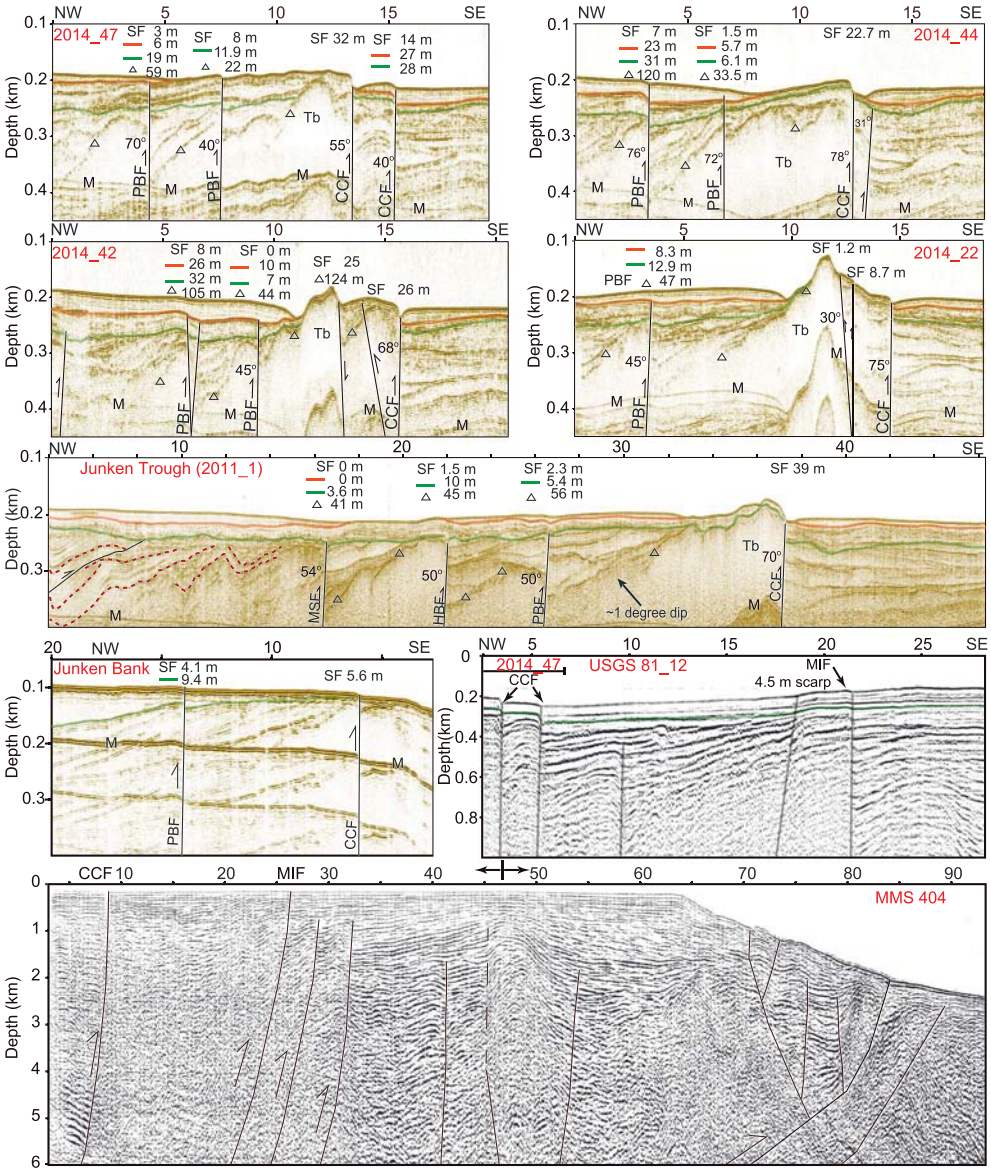

Figure 3. Northwest-southeast seismic profiles (see Figure 2 for profile locations). Green and red lines represent key boundaries, where the numbers above each fault (black lines) represent offsets for the sea floor (SF), unit I base (red line), unit II base (green), and unit III base (triangles). The numbers that lie adjacent to mapped faults represent measured fault dip. USGS 81_12 airgun profile overlaps the 2014_47 and extends across the Middleton Island fault. MMS 404 extends across the Cape Cleare fault to beyond the shelf. Tb = tertiary acoustic basement; M = sea floor multiple. Seismic profile labels are distances in kilometers. MMS = Mineral Management Services; USGS = U.S. Geological Survey. Fault abbreviations are the same as in Figure 1.

we determine that the 19.5-min (Whidbey Bay) and 20-min (Puget Bay) tsunami arrivals along the Kenai Peninsula in 1964 are consistent with motion along the Patton Bay fault (Figure 1). This fault has a clear sea floor expression and lies subparallel to the Kenai Peninsula margin (Figure 2). From bathymetric differencing, Liberty et al. (2013) found the largest scarp along the Patton Bay fault immediately southwest of Montague Island on the seafloor of the Cape Cleare Bank. There, a 40-m-deep submerged wave-cut platform experienced 8 to 12 m of uplift in 1964. Liberty et al. (2013) suggested that both the fault scarp height and amount of 1964 uplift decrease farther to the southwest.

Along the eastern margin of the Junken Trough, our new multibeam results show a 3.7-km northwest step in the Patton Bay fault scarp, as well as a step in the Cape Clear fault scarp (see below; Figure 2), suggesting

nonplane strain and likely transpressional deformation to account for an oblique fault orientation with respect to relative plate motion. The seismic data show evidence for repeated uplift along the two 40° to 70° north-dipping reverse fault segments of the Patton Bay fault, with north-dipping bedrock surfaces on both sides of the fault (Figure 3). Seismic profiles within the step-over zone show both thrust fault strands have similar slip histories (profiles 2014_47 and 2014_44; Figures S2 and S3), and these faults transition westward to a narrow kink band (2014_42; Figure S4) and single fault near the western Junken Trough margin (2014_22; Figure S5). Seismically transparent bedrock lies within 100 m of the sea floor along the length of the fault. This listric fault merges with the megathrust at about 18-km depth (Liberty et al., 2013).

Post-LGM depositional patterns suggest the greatest throw on the Patton Bay fault has remained on southern Montague Island and the adjacent Cape Cleare Bank, as in the 1964 earthquake. Whereas the Patton Bay fault on Montague Island and Cape Cleare Bank experienced upward of 10 m of uplift during the 1964 earthquake, we interpret average uplift beneath the Junken Trough, and farther west on the Junken Bank, of no more than a few meters per Holocene event. Specifically, we measure 32 m of post-LGM displacement on the central Junken Trough profile 2014_42 (Figure S4), 12.9 m of post-LGM displacement on profile 2014_22 (Figure S5), and 9.4 m of post-LGM displacement along the Junken Bank profile farther west (Figure 3). Assuming a recurrence interval of 535 years (e.g., Shennan et al., 2014), we estimate an average slip per event of about 1 m per event beneath the Junken Trough (~2 mm/year) and about 0.3 m per 500-year event below the Junken Trough (~0.6 mm/year). This estimated Holocene slip distribution is consistent with 1964 slip models (Ichinose et al., 2007; Johnson et al., 1996), which locate a large slip patch surrounding southwestern Montague Island. The long-term deformation pattern indicates the Patton Bay fault has remained strongly coupled to the PWS asperity area for most, or all, of the Holocene record. The region of the greatest slip is coincident with the location of the SMA and lies at the southern limits of the crustal duplexing interpreted from crustal seismic profiles (Figure 1; Haeussler et al., 2015; Liberty et al., 2013). Our bathymetric and seismic interpretations, coupled with tsunami travel times, strongly suggest that the Patton Bay fault near Montague Island was responsible for the early tsunami arrival on the Kenai Peninsula.

4.2. Cape Cleare Fault

Our new bathymetric data show the Cape Cleare fault forming a 69-m-high sea floor scarp on the Cape Cleare Bank (Figure 2). Bathymetric differencing indicates uplift of more than 10 m on this fault during the 1964 earthquake (Liberty et al., 2013), but there was no identified surface rupture of the Montague Island portion of the fault (Plafker, 1969). Sea floor uplift along the Cape Cleare fault increases to the southwest across the Cape Cleare Bank (Liberty et al., 2013). Although pre-1964 bathymetric measurements are sparse within the Junken Trough, our new bathymetry data are consistent with significant uplift in 1964.

Beneath the eastern Junken Trough margin, bathymetric data show a 1.8-km northwest step in the Cape Cleare fault and a series of bedrock knobs in the fault's hanging wall (Figure 2). The sparker seismic profiles define a ~70° north-dipping fault with north-dipping reflectors that lie above bedrock in the hanging wall and mostly flat-lying reflectors in the footwall (Figure 3). In addition to oblique connector faults that step between thrusts beneath the Junken Trough, folded strata between strands (profile 2014_47; Figure S2) suggest localized shortening. A backthrust and related normal fault on profile 2014_42 (Figure S4) defines a small graben. We estimate that these small thrusts and the backthrust likely merge between 1- and 2-km depths. Bedrock exposures in the hanging wall make it difficult to estimate Holocene slip rates; however, the shallow bedrock surface suggests greater Holocene slip on this fault than on the Patton Bay fault beneath the Junken Trough. Flat-lying foot wall reflectors suggest little Holocene deformation immediately south of the fault. As with the Patton Bay fault, the zone of the greatest coseismic uplift appears immediately south of the SMA (Figure 1). Although the Cape Cleare and Patton Bay faults can be mapped separately, their proximity and the number of fault step overs indicate that on a large scale, these faults should be considered together as a singular fault system where shallow slip spans two fault strands.

The 10- to 12-min delay between the first and second tsunami waves observed in Whidbey and Puget Bays is consistent with vertical sea floor displacement about 20 to 30 km farther south from the first source. While the active Cape Cleare fault is located only 10 km seaward of the Patton Bay fault, imprecise travel time observations could point to this fault as a tsunami source. Alternatively, motion on a ~100-km long, west-to-east, north-side up anastomosing sea floor scarp between the Junken Trough and Middleton Island, which we term the Middleton Island fault (Figures 1 and 2), may also be a tsunami source.

4.3. Middleton Island Fault

Plafker et al. (1978) mapped a series of faults and folds from seismic reflection data in the eastern Gulf of Alaska region. They identified faults, both north and south of Middleton Island, which likely uplifted the island during earthquakes, and tilted the island between earthquakes (Savage et al., 2014). West of Middleton Island, our legacy bathymetric map shows the Middleton Island fault as a west-trending scarp up to 23-m-high, located immediately south of, and parallel to, the SMA (Figure 1). Slip on this fault diminishes to the west, where we measure a 4.5-m-high scarp to the east of the Junken Trough (Figures 2 and 3). Plafker (1969) measured 3.5 m of uplift near the eastern limits of this fault during the 1964 earthquake, Savage et al. (2014) documented five prior earthquakes that caused 40 m of uplift of Middleton Island, and Haeussler et al. (2015) documented a major thrust fault immediately east of the island that splays from the 12–15-km-deep megathrust (Figure 1). Airgun profiles USGS 81_12 and MMS 404 show the Middleton Island fault as a 6-km-wide series of parallel thrust faults with deformed footwall strata (Figure 3). Deformation shallows along the northern fault strands, indicating a northward age progression of fault strands and that the latest fault motions are found near the SMA.

Although we did not acquire new data across this fault, scarps and faults identified from legacy seismic and bathymetric data suggest uplift west of Middleton Island likely caused the second of the 1964 tsunami arrivals in Whidbey and Puget Bays and caused the initial outflow of water for the tsunami at Middleton Island (Figure 1). We infer the Middleton Island fault has remained active throughout late Holocene time because of the large sea floor scarp with respect to single earthquake fault motion and because of the repeated uplifts documented on Middleton Island. The fault scarps terminate to the west near the Cape Cleare fault, where we observe a graben between the two fault systems and a broad anticline in the footwall block of the Middleton Island fault (Figure 3). Given the height of the sea floor scarp and slip across the LGM unconformity on profile USGS 81_12, this fault likely produced tsunamis during Holocene earthquakes. Again, this fault is located updip of, and parallel to, plate interface duplexing and the SMA (Haeussler et al., 2015; Liberty et al., 2013; Figure 1), and there is little evidence of active deformation south of this fault on the MMS 404 profile (Figure 3).

The Middleton Island fault matches the tsunami travel time and direction recorded on Middleton Island in 1964, is consistent with a fault that caused 5 m of uplift on Middleton Island in 1964 (e.g., Savage et al., 2014), and is associated with a 23-m-high sea floor scarp near the Hinchinbrook Channel, and Haeussler et al. (2014) imaged the Middleton Island fault as a splay from the megathrust (Figure 1). Tsunami genesis from this fault was likely in 1964 and will likely repeat during future earthquakes.

5. Evidence for a Long-Lived Asperity

The post-1964 plate locking above the PWS asperity (Zweck et al., 2002) suggests the same region with the largest coseismic motion in 1964 is accumulating strain for the next megathrust earthquake. Based on the deformation patterns of the splay faults, the correlation between the faulting and the region of high coupling in southern PWS and the correlation with the SMA, we suggest the PWS asperity has remained fixed throughout the Holocene, with the same faults coseismically accommodating upper-plate shortening. Thus, the impressive Patton Bay, Cape Cleare, and Middleton Island fault sea floor scarps resulted from repeating ruptures. These faults will likely produce similar uplift during future earthquakes. Regardless of the detailed slip distribution during a particular great earthquake, tsunami genesis from any of the three faults will result in travel time differences of only a few minutes.

The complex surface expressions of the identified faults lie within a narrow zone immediately seaward of the SMA, where listric thrust faults splay from the plate boundary (Figure 1; Brocher et al., 1994; Haeussler et al., 2015; Liberty et al., 2013). Conversely, the set of large subparallel surface ruptures, expressed as bathymetric scarps, are constrained to the ~150-km extent of the northwest-trending SMA. This suggests that the SMA defines the PWS asperity, and earthquakes from this asperity produce repeated tsunamigenic surface ruptures. The growth faulting indicate these faults had similar displacements during most Holocene earthquakes and that the PWS asperity therefore has persisted through most Holocene earthquakes.

Megathrust splay faulting is often exhibited near the outer ridges of accretionary prisms (e.g., Becel et al., 2017; Collot et al., 2008; Moore et al., 2007; Park et al., 2002). In contrast, we show oblique shortening along

the PWS subduction zone segment, located on the continental shelf, that is responding to a lateral transition from shallow angle subduction of the Yakutat terrane to steeper-dipping Pacific plate subduction (e.g., Brocher et al., 1994; Eberhart-Phillips et al., 2006; Kim et al., 2014). These results support the observations of Becel et al. (2017) that the morphology and structure of the subducted slab can substantially influence the pattern of shortening, splay fault generation, and tsunami generation in subduction zones. Our observations extend this observation beyond the frontal subduction zone prism.

6. Conclusions

We show evidence for repeated sea floor ruptures related to a region of high moment release of the PWS asperity. Faults that splay from the megathrust have responded with similar coseismic surface rupture patterns during Holocene time (perhaps the past 20 to 30 earthquakes). We suggest these same faults will rupture during the next megathrust earthquake, producing similar tsunami run-up and travel times as during the 1964 earthquake. Detailed sea floor and subbottom mapping from a new bathymetric and seismic survey, coupled with legacy geophysical data, provides spatial and temporal views of megathrust behaviors. We conclude that the surface expression of the splay faults is tied to plate boundary conditions, indicating a persistence of asperities during multiple earthquakes. These observations may apply to other subduction zone systems with high tsunami hazards, especially where splay faults may surface far from the trench. Mapping plate boundary and upper-plate structures is a critical step toward understanding tsunami sources in subduction zones.

Acknowledgments
The U.S. Geological Survey Earthquake Hazards Program award G11AP20143 and G13AP00021, in part, funded this work. We thank the Alaska Department of Fish and Game and R/V Solstice Captain and crew for a successful cruise. We thank David Finlayson, Alicia Balster-Gee, Gerry Hatcher, and Pete Dartnell for help with geophysical data acquisition and processing. ProMAX seismic processing software was provided by Landmark Graphics Corporation Strategic University Alliance grant agreement 2013-UGP-009000. Matthias Delescluse and Rob Witter provided improvements to this manuscript. Any use of trade, product, or firm names is for descriptive purposes only and does not imply endorsement by the U.S. Government. Legacy bathymetric data are available for download online (https://maps.ngdc.noaa.gov/). Legacy seismic data are available for download online (https://walrus.wr.usgs.gov/namss/). Seismic and bathymetric data acquired as part of this study are available online (http://www.sciencebase.gov/).

References

Atwater, B. F., & Hemphill-Haley, E. (1997). Recurrence intervals for great earthquakes of the past 3,500 years at northeastern Willapa Bay, Washington. U.S. *Geological Survey Professional Paper*, *1576*, 108. https://doi.org/10.3133/pp1576

Balster-Gee, A. F., Brothers, D. S., Finlayson, D. P., Liberty, L. M., Dartnell, P., Hatcher, G. A., et al. (2019). Bathymetry, acoustic backscatter, and minisparker seismic-reflection datasets collected southwest of Montague Island and southwest of Chenega Island, Alaska during field activity 2014-622-FA. U.S. Geological Survey Data Release. https://doi.org/10.5066/P9K1YQ35

Becel, A., Shillington, D. J., Delescluse, M., Nedimović, M. R., Abers, G. A., Saffer, D. M., et al. (2017). Tsunamigenic structures in a creeping section of the Alaska subduction zone. *Nature Geoscience*, *10*(8), 609–613. https://doi.org/10.1038/NGEO2990

Brocher, T. M., Fuis, G. S., Fisher, M. A., Plafker, G., Moses, M. J., Taber, J. J., & Christensen, N. I. (1994). Mapping the megathrust beneath the northern Gulf of Alaska using wide-angle seismic data. *Journal of Geophysical Research*, *99*(B6), 11,663–11,685. https://doi.org/10.1029/94JB00111

Brothers, D. S., Haeussler, P. J., Liberty, L., Finlayson, D., Geist, E., Labay, K., & Byerly, M. (2016). A submarine landslide source for the devastating 1964 Chenega tsunami, southern Alaska. *Earth and Planetary Science Letters*, *438*, 112–121. https://doi.org/10.1016/j.epsl.2016.01.008

Bruns, T. R. (1983). Model for the origin of the Yakutat block, an accreting terrane in the northern Gulf of Alaska. *Geology*, *11*(12), 718–721. https://doi.org/10.1130/0091-7613(1983)11<718:MFTOOT>2.0.CO;2

Carlson, P. R. (1989). Seismic reflection characteristics of glacial and glacimarine sediment in the Gulf of Alaska and adjacent fjords. *Marine Geology*, *85*(2–4), 391–416. https://doi.org/10.1016/0025-3227(89)90161-8

Carver, G., & Plafker, G. (2008). Paleoseismicity and neotectonics of the Aleutian Subduction Zone—An overview. In J. T. Freymueller, P. J. Haeussler, R. L. Wesson, & G. Ekström (Eds.), *Active tectonics and seismic potential of Alaska Geophysical Monograph Series*, (pp. 43–63). Washington, DC: American Geophysical Union. https://doi.org/10.1029/179GM03

Christensen, D. H., & Beck, S. L. (1994). The rupture process and tectonic implications of the great 1964 Prince William Sound earthquake. *Pure and Applied Geophysics*, *142*(1), 29–53. https://doi.org/10.1007/BF00875967

Cisternas, M., Atwater, B. F., Torrejón, F., Sawai, Y., Machuca, G., Lagos, M., et al. (2005). Predecessors of the giant 1960 Chile earthquake. *Nature*, *437*(7057), 404–407. https://doi.org/10.1038/nature03943

Collot, J. Y., Agudelo, W., Ribodetti, A., & Marcaillou, B. (2008). Origin of a crustal splay fault and its relation to the seismogenic zone and underplating at the erosional north Ecuador–south Colombia oceanic margin. *Journal of Geophysical Research*, *113*, B12102. https://doi.org/10.1029/2008JB005691

Eberhart-Phillips, D., Christensen, D. H., Brocher, T. M., Hansen, R., Ruppert, N. A., Haeussler, P. J., & Abers, G. A. (2006). Imaging the transition from Aleutian subduction to Yakutat collision in central Alaska, with local earthquakes and active source data. *Journal of Geophysical Research: Solid Earth*, *111*, B11303. https://doi.org/10.1029/2005JB004240

Elliott, J. L., Larsen, C. F., Freymueller, J. T., & Motyka, R. J. (2010). Tectonic block motion and glacial isostatic adjustment in southeast Alaska and adjacent Canada constrained by GPS measurements. *Journal of Geophysical Research*, *115*, B09407. https://doi.org/10.1029/2009JB007139

Enkelmann, E., Valla, P. G., & Champagnac, J. D. (2015). Low-temperature thermochronology of the Yakutat plate corner, St. Elias Range (Alaska): bridging short-term and long-term deformation. *Quaternary Science Reviews*, *113*, 23–38.

Ferguson, K. M., Armstrong, P. A., Arkle, J. C., & Haeussler, P. J. (2015). Focused rock uplift above the subduction décollement at Montague and Hinchinbrook Islands, Prince William Sound, Alaska. *Geosphere*, *11*(1), 144–159. https://doi.org/10.1130/GES01036.1

Finn, S. P. S. P., Liberty, L. M. L. M., Haeussler, P. J. P. J., & Pratt, T. L. T. L. (2015). Landslides and megathrust splay faults captured by the late Holocene sediment record of eastern Prince William Sound, Alaska. *Bulletin of the Seismological Society of America*, *105*(5), 2343–2353. https://doi.org/10.1785/0120140273

Freymueller, J. T., Woodard, H., Cohen, S. C., Cross, R., Elliott, J., Larsen, C. F., et al. (2008). Active deformation processes in Alaska, based on 15 years of GPS measurements. In J. T. Freymueller, P. J. Haeussler, R. L. Wesson, & G. Ekström (Eds.), *Active tectonics and seismic potential of Alaska* (Vol. 179, pp. 1–42). https://doi.org/10.1029/179GM02

Fruehn, J., von Huene, R., & Fisher, M. A. (1999). Accretion in the wake of terrane collision: The Neogene accretionary wedge off Kenai Peninsula, Alaska. *Tectonics*, *18*(2), 263–277. https://doi.org/10.1029/1998TC900021

Fujiwara, T., Kodaira, S., No, T., Kaiho, Y., Takahashi, N., & Kaneda, Y. (2011). The 2011 Tohoku-Oki earthquake: Displacement reaching the trench axis. *Science*, *334*(6060), 1240–1240. https://doi.org/10.1126/science.1211554

Haeussler, P. J., Parsons, T., Finlayson, D. P., Hart, P., Chaytor, J. D., Ryan, H., & Liberty, L. (2014). New imaging of submarine landslides from the 1964 earthquake near Whittier, Alaska, and a comparison to failures in other Alaskan fjords. In *Submarine mass movements and their consequences* (pp. 361–370). Cham: Springer. https://doi.org/10.1007/978-3-319-00972-8_32

Haeussler, P. J. P. J., Armstrong, P. A. P. A., Liberty, L. M. L. M., Ferguson, K. M. K. M., Finn, S. P. S. P., Arkle, J. C. J. C., & Pratt, T. L. T. L. (2015). Focused exhumation along megathrust splay faults in Prince William Sound, Alaska. *Quaternary Science Reviews*, *113*, 8–22. https://doi.org/10.1016/j.quascirev.2014.10.013

Henstock, T. J., McNeill, L. C., & Tappin, D. R. (2006). Seafloor morphology of the Sumatran subduction zone: Surface rupture during megathrust earthquakes? *Geology*, *34*(6), 485–488. https://doi.org/10.1130/22426.1

Ichinose, G., Somerville, P., Thio, H. K., Graves, R., & O'Connell, D. (2007). Rupture process of the 1964 Prince William Sound, Alaska, earthquake from the combined inversion of seismic, tsunami, and geodetic data. *Journal of Geophysical Research*, *112*, B07306. https://doi.org/10.1029/2006JB004728

Jaeger, J. M., Nittrouer, C. A., Scott, N. D., & Milliman, J. D. (1998). Sediment accumulation along a glacially impacted mountainous coastline: Northeast Gulf of Alaska. *Basin Research*, *10*(1), 155–173. https://doi.org/10.1046/j.1365-2117.1998.00059.x

Jakobsson, M., Andreassen, K., Bjarnadottir, L. R., Dove, D., Dowdeswell, J. A., England, J. H., et al. (2014). Arctic Ocean glacial history. *Quaternary Science Reviews*, *92*, 40–67. https://doi.org/10.1016/j.quascirev.2013.07.033

Johnson, J. M., Satake, K., Holdahl, S. R., & Sauber, J. (1996). The 1964 Prince William Sound earthquake: Joint inversion of tsunami and geodetic data. *Journal of Geophysical Research*, *101*(B1), 523–532. https://doi.org/10.1029/95JB02806

Kim, Y., Abers, G. A., Li, J., Christensen, D., Calkins, J., & Rondenay, S. (2014). Alaska megathrust 2: Imaging the megathrust zone and Yakutat/Pacific plate interface in the Alaska subduction zone. *Journal of Geophysical Research: Solid Earth*, *119*, 1924–1941. https://doi.org/10.1002/2013JB010581

Kopczynski, S. E., Kelley, S. E., Lowell, T. V., Evenson, E. B., & Applegate, P. J. (2017). Latest Pleistocene advance and collapse of the Matanuska–Knik glacier system, Anchorage lowland, southern Alaska. *Quaternary Science Reviews*, *156*, 121–134. https://doi.org/10.1016/j.quascirev.2016.11.026

Kuehl, S. A., Miller, E. J., Marshall, N. R., & Dellapenna, T. M. (2017). Recent paleoseismicity record in Prince William Sound, Alaska, USA. *Geo-Marine Letters*, *37*(6), 527–536. https://doi.org/10.1007/s00367-017-0505-7

Lagoe, M. B., Eyles, C. H., Eyles, N., & Hale, C. (1993). Timing of late Cenozoic tidewater glaciation in the far North Pacific. *Geological Society of America Bulletin*, *105*(12), 1542–1560. https://doi.org/10.1130/0016-7606(1993)105<1542:TOLCTG>2.3.CO;2

Liberty, L. M. (2013). Retrieval, processing, interpretation and cataloging of legacy seismic reflection data, Gulf of Alaska, US Geological Survey Final Technical Report (17 P). Retrieved from https://earthquake.usgs.gov/cfusion/external_grants/reports/G12AP20078.pdf

Liberty, L. M., Finn, S. P., Haeussler, P. J., Pratt, T. L., & Peterson, A. (2013). Megathrust splay faults at the focus of the Prince William Sound asperity, Alaska. *Journal of Geophysical Research: Solid Earth*, *118*, 5428–5441. https://doi.org/10.1002/jgrb.50372

Mann, D. H., & Peteet, D. M. (1994). Extent and timing of the last glacial maximum in southwestern Alaska. *Quaternary Research*, *42*(02), 136–148. https://doi.org/10.1006/qres.1994.1063

Misarti, N., Finney, B. P., Jordan, J. W., Maschner, H. D., Addison, J. A., Shapley, M. D., et al. (2012). Early retreat of the Alaska Peninsula Glacier Complex and the implications for coastal migrations of First Americans. *Quaternary Science Reviews*, *48*, 1–6. https://doi.org/10.1016/j.quascirev.2012.05.014

Moore, G. F., Bangs, N. L., Taira, A., Kuramoto, S., Pangborn, E., & Tobin, H. J. (2007). Three-dimensional splay fault geometry and implications for tsunami generation. *Science*, *318*(5853), 1128–1131. https://doi.org/10.1126/science.1147195

Murty, T. S. (1977). *Seismic sea waves: Tsunamis (No. 198)*, *Bulletin of the Fisheries Research Board of Canada* (Vol. 198). Department of Fisheries and the Environment, Fisheries and Marine Service. Ottawa (Canada) IX, 337 S., 331

Park, J. O., Tsuru, T., Kodaira, S., Cummins, P. R., & Kaneda, Y. (2002). Splay fault branching along the Nankai subduction zone. *Science*, *297*(5584), 1157–1160. https://doi.org/10.1126/science.1074111

Parsons, T., Geist, E. L., Ryan, H. F., Lee, H. J., Haeussler, P. J., Lynett, P., et al. (2014). Source and progression of a submarine landslide and tsunami: The 1964 Great Alaska earthquake at Valdez. *Journal of Geophysical Research: Solid Earth*, *119*, 8502–8516. https://doi.org/10.1002/2014JB011514

Plafker, G. (1969). Tectonics of the March 27, 1964 Alaska earthquake: U.S. Geological Survey Professional Paper 543–I, 74 p., 2 sheets, scales 1: 2,000,000 and 1: 500,000. Retrieved from https://pubs.usgs.gov/pp/0543i/

Plafker, G., Bruns, T. R., Carlson, P. R., Molnia, B. F., Scott, E. W., Kahler, R., & Wilson, C. (1978). Petroleum potential, geologic hazards, and technology for exploration in the outer continental shelf of the Gulf of Alaska Tertiary province. US Geological Survey Open File Report 78–490, 50 p.

Saillard, M., Audin, L., Rousset, B., Avouac, J.-P., Chlieh, M., Hall, S. R., et al. (2017). From the seismic cycle to long-term deformation: Linking seismic coupling and Quaternary coastal geomorphology along the Andean megathrust. *Tectonics*, *36*, 241–256. https://doi.org/10.1002/2016TC004156

Savage, J. C., Plafker, G., Svarc, J. L., & Lisowski, M. (2014). Continuous uplift near the seaward edge of the Prince William Sound megathrust: Middleton Island, Alaska. *Journal of Geophysical Research: Solid Earth*, *119*, 6067–6079. https://doi.org/10.1002/2014JB011127

Shennan, I., Bruhn, R., Barlow, N., Good, K., & Hocking, E. (2014). Late Holocene great earthquakes in the eastern part of the Aleutian megathrust. *Quaternary Science Reviews*, *84*, 86–97. https://doi.org/10.1016/j.quascirev.2013.11.010

Shugar, D. H., Walker, I. J., Lian, O. B., Eamer, J. B., Neudorf, C., McLaren, D., & Fedje, D. (2014). Post-glacial sea-level change along the Pacific coast of North America. *Quaternary Science Reviews*, *97*, 170–192. https://doi.org/10.1016/j.quascirev.2014.05.022

Sieh, K., Natawidjaja, D. H., Meltzner, A. J., Shen, C. C., Cheng, H., Li, K. S., et al. (2008). Earthquake supercycles inferred from sea-level changes recorded in the corals of west Sumatra. *Science*, *322*(5908), 1674–1678. https://doi.org/10.1126/science.1163589

Taliaferro, N. L. (1932). Geology of the Yakataga, Katalla, and Nichawak districts, Alaska. *Bulletin of the Geological Society of America*, *43*(3), 749–782. https://doi.org/10.1130/GSAB-43-749

Zweck, C., Freymueller, J. T., & Cohen, S. C. (2002). Three-dimensional elastic dislocation modeling of the postseismic response to the 1964 Alaska earthquake. *Journal of Geophysical Research*, *107*(B4), 2064. https://doi.org/10.1029/2001JB000409